Directed dynamic self-assembly of objects rotating on two parallel fluid interfaces

Bartosz A. Grzybowski[a] and George M. Whitesides[b]
Department of Chemistry and Chemical Biology, Harvard University, Cambridge, Massachusetts 02138

(Received 12 October 2001; accepted 28 January 2002)

This paper describes dynamic self-assembly of millimeter-sized objects rotating at two parallel fluid interfaces and interacting with one another hydrodynamically, both in the plane of the interface and between the interfaces. The nature of hydrodynamic interactions between the objects rotating on different interfaces and, consequently, the morphologies of the ordered structures that self-assemble, depend on the sizes and the three-dimensional shapes of the rotating particles. Large particles rotating on one interface (''templates'') can direct the self-assembly of smaller particles (''substrates'') on the other interface. Two examples of directed self-assembly are discussed: (i) selective dimerization of disk spinning on the lower interface under the influence of cylinders rotating on the upper interface, and (ii) assembly of ''substrate'' rectangles into a pattern of squares that is identical with the pattern formed by the ''template'' squares. General, qualitative characteristics of the vortex–vortex interactions between objects of complex shapes are discussed. [DOI: 10.1063/1.1462607]

I. INTRODUCTION

Dynamic self-assembly (DySA),[1,2] that is, self-assembly in nonequilibrium systems[3,4] that organize only when dissipating energy, is a promising strategy of preparing adaptive[5,6] structures (or materials), whose internal organization and properties could be controlled by the amount of energy delivered to the system externally. Such structures could have applications in photonics (e.g., as tunable optical elements[7,8]), and in micromechanical devices[9] (as sensors or reconfigurable machines).

We have recently described[10] a dynamic system in which millimeter-sized, magnetized disks rotate at two parallel fluid interfaces under the influence of a rotating external magnetic field, and interact with one another through the vortices they create in the surrounding liquid. In this system, all disks spin with angular velocity ω equal to that of the external magnet, and are attracted towards its axis of rotation by a centrosymmetric magnetic force F^m. The hydrodynamic interactions between the disks spinning at one interface are repulsive,[11–13] while those between disks spinning at different interfaces are repulsive at low rotational speeds, and attractive at high values of ω. The interplay between the magnetic and hydrodynamic forces leads to the formation of ordered aggregates whose dimensions and morphologies can be tuned by adjusting ω.

Here, we describe an analogous systems in which magnetized objects that self-assemble at one (''control'') interface direct the self-assembly of objects—magnetized or nonmagnetized, depending on the design of the system—floating at a parallel (''production'') interface. We show that the vortex–vortex interactions between the interfaces can be modified by changing the shapes, magnetic loadings, or rotation rates of the spinning particles, and can control the morphologies of structures that form at the ''production'' interface. We describe two examples of directed DySA achieved by engineering vortex–vortex interactions: (i) formation of a pattern of dimers of rotating, magnetized disks at the ''production'' interface under the influence of strong vortices produced by an array of tapered cylinders spinning at the ''control'' interface; (ii) self-assembly of a pattern of squares from non-magnetic rectangles caused by the vortices generated by an isomorphic pattern of rotating, magnetized squares. We qualitatively describe the hydrodynamic forces that lead to the formation of these assemblies, and abstract principles that can guide design of other directed-DySA systems based in vortex–vortex interactions.

II. EXPERIMENT

Figure 1(a) outlines the experiment. A permanent bar magnet of dimensions 5.6 cm×4 cm×1 cm rotated with angular velocity ω (~500–1000 rpm) below a dish filled with two immiscible liquids forming two layers: the bottom layer of perfluorodecalin (PFD), and the top layer of 3:1 by volume solution of ethylene glycol and water (EG-H_2O).[14] The magnet was magnetized along its longest dimension and had magnetization $M \sim 1000\ \mathrm{G/cm^3}$. The distance between the upper face of the magnet and the PFD/EG-H_2O interface was $H \sim 30$ mm, and the thickness of the EG-H_2O layer was $h \sim 3$ mm.

The circular disks were fabricated by a two-step procedure. First, a hollow polyethylene tubing (~1 mm i.d., ~2 mm o.d., Intramedic) was filled with poly(dimethylsiloxane) (PDMS, Dow Corning) doped with magnetite (15% by weight), and the polymer was allowed to cure at 60 °C for 2 h. The resulting composite was cut into slices ~400 μm thick using a custom-made precision cutter.[15] Disks were placed on PFD/EG-H_2O and EG-H_2O/air interfaces, and were fully immersed in the EG-H_2O layer.

[a]Electronic mail: bgrzybowski@concurrentpharma.com
[b]Electronic mail: gwhitesides@gmwgroup.havard.edu

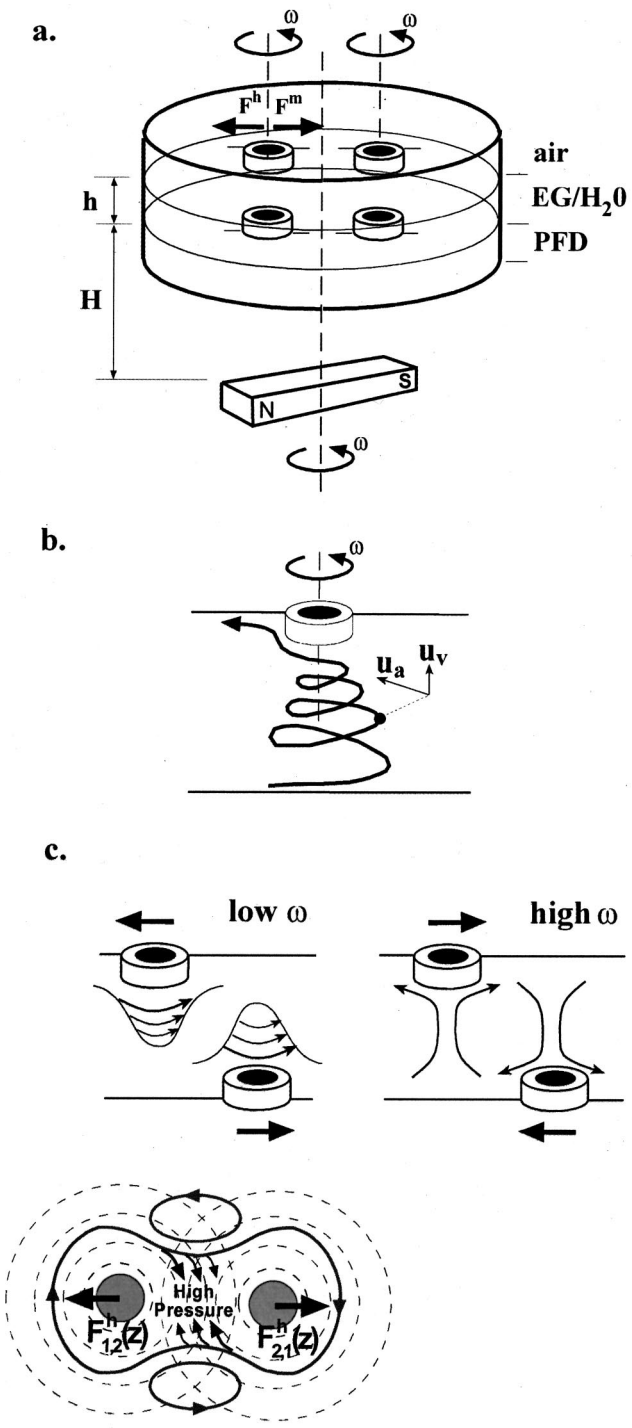

FIG. 1. (a) Shows the scheme of the experimental arrangement. The magnetic and hydrodynamic forces acting on disks spinning on the same interface are indicated. The schematic picture in (b) illustrates the motion of liquid elements along a helical streamline under a disk rotating on the EG/air interface. The horizontal azimuthal (u_a) and vertical (u_v) components of velocity of a fluid element on this streamline are shown in the insert. (c) At low rotational speeds (left picture), the magnitude of the azimuthal component of velocity within a Taylor vortex is larger than the vertical component. Consequently, interaction between the disks spinning on different interfaces is qualitatively similar to that between two disks spinning on the same interface. The origin of this repulsive interaction is illustrated in the bottom picture. At high rotational speeds (right picture), the vertical component of velocity is large. The fluid is pumped from the lower interface onto the upper disk, and from the upper interface onto a lower disk. The disks move towards each other in response to the pressure gradients established at each interface.

The magnetized squares were fabricated by molding PDMS/magnetite mixture (~6:1 by weight) against a glass master having an array of rectangular depressions (2 mm $\times$2 mm$\times$1 mm) embossed on its surface. The polymer was cured thermally at 60 °C for 2 h, and the objects were released by soaking them in chloroform for 10 min. The wettabilities[16] of the faces of the resulting pieces were modified according to the following procedure: (i) the faces that were to remain hydrophobic were painted with a xylene-based paint; (ii) the unpainted faces were made hydrophilic by plasma oxidation of the pieces for 1 min; (iii) the xylene paint was removed by rinsing the objects with hexanes. In particular, two kinds of magnetic squares were prepared. In the first type, all but one (bottom square) face were made hydrophilic, so that the squares floated parallel to the PFD/EG-H_2O interface, and did not form discernible menisci at their side, rectangular faces [cf. Fig. 3(a)]. In the second type, two of the side faces were made hydrophobic [cf. Figs. 3(b), 3(c)], and the squares were tilted with respect to the PFD/EG-H_2O interface. The hydrophobic faces were partly immersed in the PFD layer; small menisci formed at the parts of these faces above the plane of the interface.

White, nonmagnetic rectangles were made of PDMS doped with 1% by weight silica powder, and were prepared by molding against a master with rectangular (2 mm $\times$1 mm$\times$1 mm) depressions on its surface. The rectangles were cured thermally, and were subsequently exposed to oxygen plasma for 1 min, so that all their faces were made hydrophilic. When placed at the EG-H_2O/air interface, these rectangles were fully immersed in the liquid except for their top surface.

All experiments were started from random initial configurations of the particles. The particles were placed onto appropriate interfaces when the permanent magnet was stationary. Introduction of magnetic objects onto the interfaces in the presence of the rotating magnetic field was also possible, but it occasionally made orienting them (e.g., putting ''flat'' onto the interface) more difficult.

The images of the aggregates were taken with a CCD camera interfaced to a VHS recorder and were subsequently digitized using ScionImage software. The flowlines in the EG-H_2O layer were visualized by adding droplets of a solution of Crystal Violet in 3:1 by volume mixture of ethylene glycol and water.

III. DESCRIPTION OF THE FORCES ACTING IN THE SYSTEM

A. Forces acting within one layer

Under the influence of the magnetic field produced by the rotating magnet, all magnetically doped particles floating at either of the two interfaces experience a centrosymmetric force F^m directed towards the axis of rotation of the magnet. With the magnet used in our experiments, and for distances between the top face of the magnet and an interface H ~3 cm, this magnetic force is a slowly varying function of position within an interface.[12] Also, if the distance h between the interfaces is small, the value of this force is approximately equal on both interfaces.

In the plane of the interface, rotating objects interact with one another by repulsive hydrodynamic forces [Fig. 1(a)]. We have previously suggested[11,12] that the origin of these repulsions can be explained using ideas from low-(but not zero)-Reynolds-number hydrodynamics. We showed[12] that for interacting disks, the hydrodynamic repulsion F_{ij}^h exerted by a disk of radius a_j on a disk of radius a_i depends on the radii of the disks, the distance d_{ij} between their centers, the rotational speed ω, and the density of the fluid ρ: $F_{ij}^h \propto \rho\omega^2 a_j{}^3 a_i{}^4/d_{ij}^3$. The force on disk *i* acts along the direction of d_{ij} and away from disk *j*. We verified experimentally that qualitatively similar relationship describes repulsions between symmetric, polygonal plates (e.g., squares, hexagons) rotating at $\omega \gtrsim 200$ rpm (the radii of the disks are replaced by the distances from the center of rotation to the vertex of a plate).

The magnitudes of the magnetic dipole–dipole forces F_{ij}^m acting between the rotating objects are small compared to the centrosymmetric magnetic force F_m and to the pairwise hydrodynamic interactions F_{ij}^h. In the presence of the external magnetic field, each magnetically-doped particle acquires a magnetic dipole of magnitude $m=\mu_0 V\chi H$, where μ_0 is the magnetic permeability of vacuum, V is the volume of a particle ($\sim$1.3 mm^3), χ is its effective magnetic susceptibility, and H is the strength of the magnetic field in the plane of the interface ($\mu_0 H \sim 0.05$ T). Assuming that the magnetite grains are uniformly distributed in the PDMS matrix and no long-range order exists between magnetic domains (so that rotating objects are superparamagnetic rather than ferromagnetic), the value of χ can be estimated from a low-field expansion of the Langevin function,[17] $\chi(2\chi+3)/(\chi+1) = \pi\phi\mu_0 M_s^2 l^3/6kT$. In this equation, ϕ is the volume fraction of magnetite in the disks ($\sim$0.01), M_s is the saturation magnetic moment of magnetite ($\sim 0.4\times 10^6$ A/m), and l is the typical size of a magnetite grain ($\sim$100 Å). The value of χ is estimated at $\sim$0.1, and the induced magnetic moment is $m \sim 6.5\times 10^{-12}$ T m^3. The magnitude of the force F_{ij}^m acting between the spinners is calculated by taking the gradient of the interparticle potential, $|F_{ij}^m| = |\partial U(r,\theta)/\partial r| = |(3m^2/4\pi\mu_0)\cdot[(1-3\cos^2\theta)/r^4]|$, where r is the distance between the centers of the particles, and θ is the angle between the line joining these centers and the direction of the external field. The magnitude of this force does not exceed $\sim$0.002 dyn, which is negligible compared[10] to magnitudes of both F_m (typically, $\sim$0.07 dyn) and F_{ij}^h (typically, several tenth of a dyne).

Objects fully immersed in the EG-H_2O layer with the exception of their top/bottom faces (i.e., disks, nonmagnetic rectangles, ''flat'' magnetic squares) did not form discernible (at the level of $\sim$100 μm) menisci. Consequently, the capillary interactions[16] between these objects were negligible: when put onto the interface in close proximity to one another, they did not clump.

The ''tilted'' magnetic squares had menisci at two of their side faces [Figs. 3(b)–3(c)], and in the absence of external, rotating magnetic field attracted one another. When these squares rotated, however, the squares separated and formed polygonal patterns similar to those formed by ''flat'' squares having no menisci [Fig. 3(a)]. Based on our previous results of finite element modeling of capillary interactions between floating particles of complex shapes,[16] we estimated the magnitude of the capillary attraction between two stationary, tilted disks separated by $\sim$10 mm [cf. Fig. 3(b)] to be $\sim$0.03 dyn, that is, small compared to the magnitude of F_{ij}^h. We further note that the magnitude of the capillary force between the *rotating* squares might be even smaller than this estimate; we observed that menisci on the faces of a rotating particle are much less pronounced than those on an identical but stationary particle. We are currently studying this effect.

B. Forces acting between the layers

The vortices produced by objects spinning on either of the two interfaces extend into the EG-H_2O layer in the direction perpendicular to the plane of the interface. The streamlines within these so-called Taylor vortices[18] trace spiral paths directed towards the interface on which the object is floating [Fig. 1(b)]; any fluid element within the vortex has azimuthal and vertical velocity components. In our previous work,[10] we suggested that hydrodynamic, ''vertical'' forces F^v between objects spinning on proximate interfaces are mediated by Taylor vortices these objects generate. Specifically, we argued that the azimuthal components of velocity (i.e., parallel to the plane of the interface, and tangential to the flowlines) in each Taylor vortex give rise to repulsive interactions between the spinning particles, while the vertical motions of the fluid (i.e., pumping of the fluid towards the spinning particle) account for the attraction between them. At low values of rotational speeds, the magnitude of the vertical component is small, and the objects on different interfaces interact repulsively [Fig. 1(c), left] through a lift force similar to that acting between disks spinning on one interface; the repulsion decreases (approximately exponentially) with increasing ω. At the same time, the vertical component of velocity increases monotonically with increasing ω, and so does the attraction between the spinning particles [Fig. 1(c), right]. At high rotational speeds ($\omega \gtrsim 800$ rpm) identical objects rotating on different interfaces assemble into pairs ''connected'' by a columnar vortex.

IV. SELF-ASSEMBLING SYSTEMS

A. Self-assembly of dimeric structures

We sought to engineer the vertical vortex–vortex interactions that would allow preparation of structures more complex than pairs of disks. In particular, we wished to achieve a simple transformation (''reaction'') in which disks (here, 1.57 mm in diameter) spinning on one interface (''substrates'') would form dimers under the influence of magnetized objects spinning on the other interface (''templates''). We required that this transformation should be selective, in the sense that one template would dimerize exactly two substrates, and that all available substrates would dimerize.

We modified the vortex–vortex interactions between templates and substrates by adjusting size and shape of the templates. We have previously shown[10] that for disks of the same dimensions spinning on different interfaces, the magnitude of the vertical interaction between them increases with increasing diameters of these disks. We reasoned that if

the templates were made larger than the substrates, they would be able to attract more than one substrate disk. We tested template disks of several sizes (from ~1.2 to ~3 times larger than substrate disks), and observed aggregation of several disks under one template. We found, however, that the numbers of substrates that were attracted could not be controlled; in all cases, one substrate disk occupied the position coinciding with the axis of rotation of the template, while the numbers of disks in the shell around it varied. The large template disk and the central substrate disk were joined by a localized, columnar vortex [Fig. 2(a), left] that imparted centrosymmetric forces on other disks rotating on the PFD/EG-H_2O interface. Because of this radial symmetry, several (from one to five) substrates could fit into a shell around the ''pinned'' substrate—it was impossible to engage *exactly* one disk.

We achieved selective dimerization by reducing the symmetry of the vortex produced by the template. We reasoned that if this vortex—instead of being ''conical'' and focusing towards the PFD/EG-H_2O interface [Fig. 2(b), left]—were more diffuse, the attractive force would act on substrates over a larger area of the interface, and more than one ''pinned'' disk could be drawn under the template.

The templates [Fig. 2(a), right] were made of the same tubing as the substrates, but were cut to be thicker (~2 mm), and their ends were slanted at an angle of ~30°, with respect to each other. Under the influence of the magnetic field, they spun such that their lower ends swept an area approximately twice as large as the cross section of the tubing they were made from. This sweeping motion created large patches of vorticity in the plane of the PFD/EG-H_2O interface. Although for all rotational speeds, the rate of liquid transfer towards the EG-H_2O/air interface—and thus the attraction exerted on the substrates—was ~40% lower than in experiments using disks as templates, it occurred over a larger area, into which several disks could be drawn [Fig. 2(b), right].

Figure 2(c) illustrates dimerization of 1.57 mm disks spinning on the lower interface caused by the templates (dyed white) spinning on the upper interface. At low rotational speeds ($\omega \sim 500$ rpm), the repulsions between the substrates were small, and varying numbers (up to five) of substrate disks could accommodate into broad vorticity patches created by the templates. When the rotational speed was increased to ~800 rpm, and the repulsions between the substrates grew, each template had two (usually) or three (sporadically) substrates associated with it—none of them, however, pinned on the axis of rotation of the template. If necessary, the redundant third disk was removed by increasing ω further to ~1000 rpm, so that each template had only two disks left—one near the axis of rotation of the template, and the other precessing around it [indicated by dashed lines in Fig. 2(c)]. When the rotational speed was slowly decreased back to 800 rpm, the precessing disk was drawn onto the template, to give a dimer of closely-spaced disks. These dimers were stable and no more disks were attracted onto them—the repulsion they exert on their neighbors on the same interface exceeds the attractive force produced by the template. We verified that the dimerization process is not only selective, but also exhaustive in the sense that all available substrates are dimerized [Fig. 2(d)].

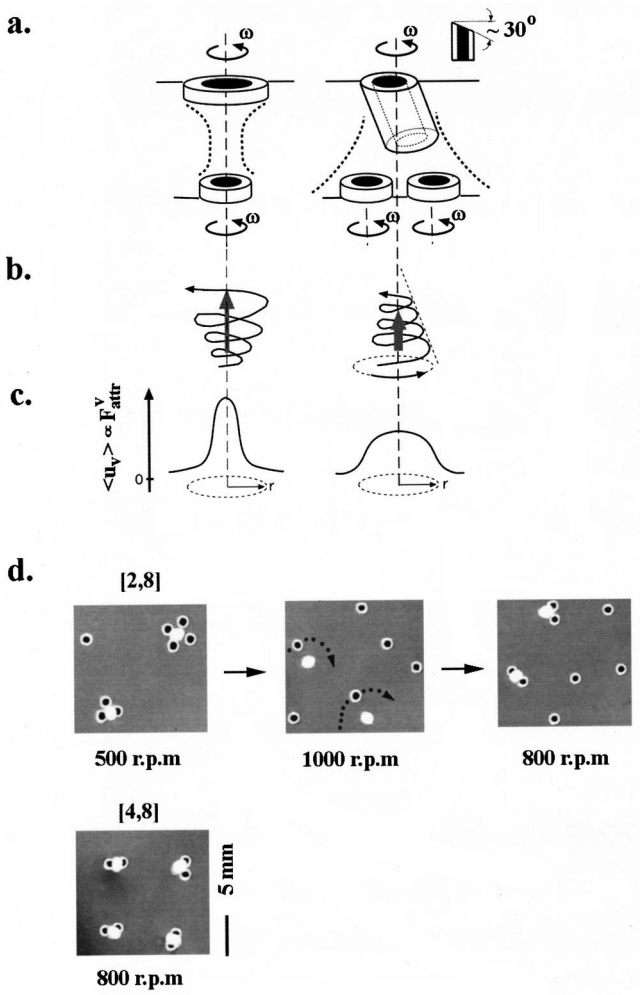

FIG. 2. Illustrates the effects of the shape of the templates on the selectivity of directed self-assembly. (a) When large disks are used as templates they ''pin'' one substrate disk under them (left picture); slanted cylinders create larger vorticity patches on the lower interface, and can selectively bind two substrate disks (right picture). (b) Shows schematically the flowlines within the vortices generated by rotating disks (left) and slanted cylinders (right). The corresponding *qualitative* radial distributions of the vertical components of velocity in these vortices are shown in (c). The formation of dimers of disks (1.57 mm in diameter) spinning on the lower interface under the influence of vortices produced by slanted-cylinder templates spinning on the upper interface is shown in (d). At low ω (~500 rpm), the number of disks attracted by a template varied—a representative example of this situation for a ^{2,8} aggregate is shown in the picture on the left. When ω was increased to ~1000 rpm, each template had exactly one disk below it, and another disk orbited around it (indicated by dashed lines). When the rotational speed was decreased to ~800 rpm, the orbiting disk was attracted towards the template, and a stable dimer formed. Exactly two disks were associated with each template. The lower picture illustrates the situation, in which the number of disks was twice that of the number of templates; all available disks were dimerized by the templates.

B. Pattern replication

We extended the principles of design of vortex–vortex interactions described in the previous section to construct a system that not only self-assembles, but also copies itself.

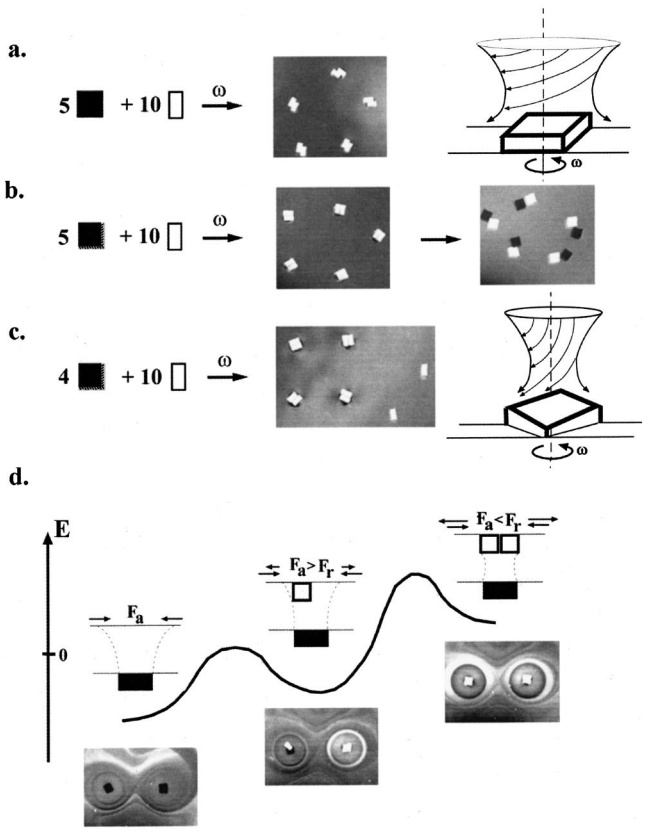

FIG. 3. (a) Illustrates the process of pattern replication using vortex–vortex interactions. In these experiments, magnetically doped squares (2 mm $\times$2 mm$\times$1 mm) were spinning on the PFD/EG-H_2O interface at $\omega \sim 700$ rpm, and were used as templates to organize nonmagnetic PDMS rectangles (2 mm$\times$1 mm$\times$1 mm) on the EG-H_2O/air interface into a pattern of squares. The EG layer was 2.5 mm thick. In (a), the rectangles formed a pentagon of dimers, in which the rectangles were slid with respect to each other. (b) When the squares had two of their faces made hydrophobic, so that they were slightly tilted with respect to the PFD/EG interface, the rectangles organized into squares. These squares remained stable, even when the magnetic field was switched off. The picture in (c) shows that the replication process is selective; when the number of building blocks (rectangles) is larger than twice that of the templates (squares), the redundant rectangles are left unused. The graph in (d) suggests a schematic energy diagram of the replication process; the inserted pictures visualize the flow lines corresponding to the energy minima.

We wanted to use objects spinning on one interface to create its own replica from smaller particles floating on the other interface.

In this system (Fig. 3), an aggregate of N magnetically doped squares ($2\times2\times1$ mm) spinning at the PFD/EG water interface organized $2N$ nonmagnetic rectangles ($2\times1\times1$ mm) floating on the upper interface into N squares; the pattern replicated at the upper interface was the copy of the pattern formed by templates at the lower interface. We used nonmagnetic objects as substrates because under the influence of the vortices produced by templates they rotated slowly ($\sim$100 rpm), and could thus come into intimate contact (had these objects been magnetized, the hydrodynamic repulsions would prohibit them approaching each other). Also, we used squares and rectangles rather than e.g., half-circles and circles, because substrates of other shapes did not assemble in unique orientations replicating the shape of the template.

The squares (templates) were made of magnetically doped PDMS, and the rectangles (substrates)—from nonmagnetic PDMS. The substrates had their surface made hydrophilic, so that in the absence of the external magnetic field they did not interact with each other through capillary forces. The thickness of the EG layer was adjusted to $h = 3$ mm. When the field was turned on ($\omega \sim 500$ rpm), the magnetized templates started spinning. The vortices generated by the templates attracted the substrates floating on the upper interface. After $\sim$5 min, all rectangles on the upper interface organized into dimers, each dimer spinning in the vortex produced by a template below it. Within each dimer, the rectangles were slightly displaced with respect to each other [Fig. 3(a)]. In order to assemble the rectangles into proper squares [Fig. 3(b), middle], the templates had two of their faces made hydrophilic, so that they were tilted with respect to the interface; this orientation increased the vertical (''attractive'') component of velocity in the vortex, and the substrates were drawn more towards the center of the vortex to form proper squares. When the field was slowly turned off, the replicated squares remained stable on the upper interface [Fig. 3(b), left]. We confirmed that the replication process is exhaustive (all magnetic templates produce a corresponding dimer on the upper interface provided that there are enough substrates), and selective [N templates use exactly $2N$ substrates, leaving extra substrates unused for replication; Fig. 3(c)].

The replication process is the consequence of the interplay between (i) the attraction of the nonmagnetic substrates towards the vortex produced by the templates, and (ii) the hydrodynamic repulsion between the substrates rotating under the influence of templates. Initially, when a template has no substrates associated with it [Fig. 3(d), left], the only interaction experienced by the substrates is the attraction towards the vortex produced by the template. We visualized this situation [left insert in Fig. 3(d)] by adding dye tracers onto the upper interface; dye is carried towards the center of the vortex. When a template engages one substrate, the substrate starts spinning under the influence of the vortex. This spinning results in a repulsive hydrodynamic force acting on other substrates floating on the upper interface (the nature of this force is identical to that between two magnetic disks spinning on one interface, cf. Fig. 1). The repulsion is, however, smaller than the attraction by a template, so that one more substrate can be engaged. When this happens, the dimer spinning in the vortex produces hydrodynamic repulsive force that offsets the attraction by the template vortex. Consequently, no more substrates can be engaged, and the replication is complete.

The increasing hydrodynamic repulsion is visualized in the inserts in Fig. 3(d). A dark circle around the spinning objects is the dye transferred onto the lower interface. On the upper interface, the dye is expelled from around the spinning substrates; this effect shows in the form of light rings in the pictures. Note that a ring is clearer around a dimer of substrates than around a single spinning substrate.

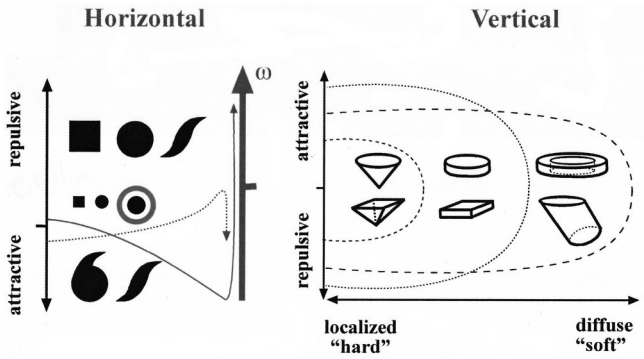

FIG. 4. Summary of horizontal and vertical vortex–vortex interactions. In the plane of the interface (left), the interactions are attractive only between asymmetric (with respect to the direction of rotation) plates rotating at low rotational speeds (dashed gray line; see Ref. 13 for details). For other shapes, interactions are repulsive for all values of ω, and depend on the size of the particles, and on their rotational speeds. Larger particles can be made to spin less rapidly—and thus repel less strongly—if they are partly made of nonmagnetic material (gray ring), with a smaller magnetic particle inside. The magnetic spinner rotates with ω equal to that of the external magnet, but the outside ring rotates more slowly. Interactions between objects at parallel, proximal interfaces (right) are repulsive for low ω, and attractive for high ω. If the vortices focus towards the proximal interface, the interactions are highly localized, if they diverge—the interactions act over larger areas. Examples of shapes of the plates that give rise to "hard" and "soft" interactions are shown in the picture. The qualitative assessments of the strengths of these interactions (dashed lines) are based on the observed rates of pumping (i.e., the rates of transfer of the fluid towards a spinning particle).

V. ENGINEERING HYDRODYNAMIC INTERACTIONS IN 2D AND 3D

The remarkable feature of the vortex–vortex interactions that mediate directed self-assembly in our system, is that they can be easily modified—both in plane of the interface, and between the interfaces—by changing the dimensions, shapes or material properties of the rotating particles. In principle, the horizontal and vertical hydrodynamic forces can be tuned selectively. In the example of dimerization we described, the interactions between the tapered cylinders in the plane of the EG-H_2O/air interface were similar to those between thin disks of the same diameters. The vertical interactions between the tapered cylinders and substrate disks on the PFD/EG-H_2O interface were, however, qualitatively very different from those acting in a system in which disks were used as templates. This ability to engineer horizontal and vertical forces *independently* of each other, suggests that the directed DySA based on vortex–vortex interactions can be a very flexible method for organizing and/or manipulating macroscopic particles.

The qualitative characteristics of hydrodynamic interactions in the plane of the interface (2D) and between the interfaces (3D) are summarized in Fig. 4. The 2D interactions are attractive only between objects that are chiral with respect to the interface and rotate at $\omega \lesssim 400$ rpm. Two examples of such objects—the comma-shaped and the propeller-shaped plates—are shown in the lower left part of Fig. 4; the detailed discussion of the hydrodynamic forces between chiral spinners is given elsewhere.[13] Achiral spinners and chiral spinners rotating at $\omega \gtrsim 400$ rpm interact with one another repulsively. The magnitude of the repulsive force increases with the sizes of interacting particles and with their rotational speeds. In multicomponent spinners, the rotational speeds of the objects can be adjusted independently of the rotational speed of the magnetic field. For instance, in the "core-and-shell" structure shown in Fig. 4, the nonmagnetic ring (gray) rotates more slowly than the magnetic particle (black) inside it; despite its large overall size, this multicomponent particle exerts low hydrodynamic repulsion on its neighbors.

Hydrodynamic forces acting between interfaces depend on the angular velocities and the three-dimensional shapes of the rotating particles (Fig. 4, right). These forces are repulsive for low ω, and attractive for high ω. If the spinning particles have conical or pyramidal shapes, they produce vortices that "focus" towards the proximal interface, and in which the vertical components of velocity are small. Consequently, the 3D interactions these particles give rise to are highly localized ("hard"), and their magnitudes are small. Planar spinners—that is, plates having their upper and lower surfaces parallel to the planes of the interfaces—pump liquids rapidly, and the vortices they create are rather diffuse; these spinners generate strong but poorly localized 3D forces. Finally, weak and highly delocalized ("soft") interactions are created by spinners that produce very diffuse vorticity patches, e.g., toroidal or tapered-cylinder spinners. Certainly, this short list is not exhaustive, and other shapes and types of forces could be considered.

VI. CONCLUSIONS AND OUTLOOK

Hydrodynamic vortex–vortex interactions can be used to self-assemble rotating, macroscopic particles in two and in three dimensions. These interactions can be easily modified, and can lead to assemblies of many different topologies. The two examples of self-assembling systems and the qualitative characteristics of vortex–vortex forces we presented, are the first step toward developing a "chemical" methodology of 3D macroscopic "synthesis" based in these forces. At present, such methodology can only be developed on the level of approximate scaling arguments. We hope, however, that our work will stimulate theoretical research on 3D multivortex flows,[19–21] and that Navier–Stokes equations describing the flows around rotating particles of complex shapes will eventually be solved.

The systems of spinning objects can serve as precursors for open 3D lattices to be used in, for example, photonic devices. We are already working with ensembles of spinners ~ 100 μm in diameter, and we verified that hydrodynamic repulsions between rotating particles are effective between ~ 25 μm spinners. The major difficulty in miniaturizing the system, is the placement of the particles onto the interface such as to avoid the capillary interactions between them. This complication would not be present, if one could stably levitate and rotate particles fully submerged in the liquid. Since stable levitation of ferromagnetic particles in the magnetic field is impossible, other ways of inducing rotations of the particles (e.g., by rotating electric or optical fields) should be considered. Finally, we believe that the aggregates of rotating magnetized objects might find uses in engineering

to power small machines. We are currently studying systems of gear-shaped plates in this context, and use vortex–vortex interactions between gears rotating at different interfaces to connect them by ''fluidic shafts.''

[1] A. S. Mikhailov and G. Ertl, Science **272**, 1596 (1996).
[2] M. C. Cross and P. C. Hohenberg, Rev. Mod. Phys. **65**, 851 (1993).
[3] P. Glansdorff and I. Prigogine, *Thermodynamic Theory of Structure, Stability, and Fluctuations* (Wiley–Interscience, New York, 1971).
[4] G. Nicolis and I. Prigogine, *Exploring Complexity* (Freeman, New York, 1989).
[5] F. Kannari, N. Takei, and M. Shiozawa, Rev. Laser Eng. **28**, 479 (2000).
[6] P. Alstrom and D. Stassinopoulos, Phys. Rev. E **51**, 5027 (1995).
[7] B. A. Grzybowski, D. Qin, and G. M. Whitesides, Appl. Opt. **38**, 2997 (1999).
[8] B. A. Grzybowski, D. Qin, R. Haag, and G. M. Whitesides, Sens. Actuators A **A86**, 81 (2000).
[9] J. J. Yao, J. Micromech. Microeng. **10**, R9 (2000).
[10] B. A. Grzybowski and G. M. Whitesides, J. Phys. Chem. B **106**, 1188 (2002).
[11] B. A. Grzybowski, H. A. Stone, and G. M. Whitesides, Nature (London) **405**, 1033 (2000).
[12] B. A. Grzybowski, X. Jiang, H. A. Stone, and G. M. Whitesides, Phys. Rev. E **6401**, 1603 (2001).
[13] B. A. Grzybowski and G. M. Whitesides, Science (in press).
[14] Kinematic viscosity of the mixture effected the stability of the aggregates. In liquids of low viscosities ($v \lesssim 3$ cp), the flows created by spinning disks were often turbulent, and the self-assembled aggregates were unstable. If the viscosity was too high ($v \gtrsim 50$ cp), the magnetic torque was to small to spin the disks. Most stable structures were observed in liquids of intermediate kinematic viscosities, such as the 1:1 mixture of EG and water.
[15] The cutter was build from three translational stages. Two of the stages were stacked on top of each other and served as an *xy* platform, on which the tubing was placed. The third stage was free to move in the direction perpendicular to the plane of the platform, and had a fine razor blade glued to it; this blade was used to cut the tubing.
[16] B. A. Grzybowski, N. Bowden, F. Arias, H. Yang, and G. M. Whitesides, J. Phys. Chem. B **105**, 404 (2001).
[17] R. E. Rosensweig, *Ferrohydrodynamics* (Dover, New York, 1997).
[18] D. J. Tritton, *Physical Fluid Mechanics* (Clarendon, Oxford, 1988).
[19] D. Dijkstra and G. J. F. Van Heijst, J. Fluid Mech. **128**, 123 (1983).
[20] T. H. Havelock, Philos. Mag. **11**, 617 (1931).
[21] D. G. Dritschel, J. Fluid Mech. **157**, 95 (1985).